Wildfire Spread Modeling with Aerial Image Processing

Qiyuan Huang, Abolfazl Razi, Fatemeh Afghah, Peter Fule School of Informatics, Computing and Cyber Systems, Northern Arizona University, Flagstaff, AZ, USA Emails: {qh33, abolfazl.razi, fatemeh.afghah, pete.fule}@nau.edu

Abstract—Currently, wildfire spread modeling has drawn a lot of attention from the research community since many countries are suffering from severe socioeconomic impacts of wildfires, every year. Fire spread modeling is a key requirement for effective fire management to deploy fire control equipment and forces at the right time and locations, and plan timely evacuations of residential areas.

This paper proposes a new data-driven model for fire expansion which uses reference-based image segmentation for vegetation density estimation and incorporates it into the fire heat conduction modeling. Compared with the conventional parameter collection methods at fire scenes, our method relies on topview images taken by unmanned aerial vehicles, which provides significant advantages of flexibility, safety, low cost, and convenience. Our low-complexity and probabilistic model incorporates the terrain slope, vegetation density, and wind factors with adjustable model parameters which can be easily learned from experiments. The proposed model is flexible and applicable to forests with mixed vegetation and different geographical and climate conditions. We evaluate the fire propagation model by comparing the results with the propagation data available for California Rim fire in 2013 ¹.

I. INTRODUCTION

Wildfire is a growing threat to humankind with severe socioeconomic impacts. In 2018 alone, more than 58,000 fires burned nearly nine million acres across the United States. More than 25,000 structures were destroyed, including 18,137 residences and 229 commercial structures [1]. This threat is not specific to the USA. In Australia, the bushfires have been destructive in many ways. During the 2019-2020 season, more than 46 million acres (72,000 square miles) of land were burned and at least 34 people died in the bushfires [2]. Wildfires also lead to devastating damage to the environment. At least 80 percent of the Blue Mountains World Heritage area in New South Wales and 53 percent of the Gondwana world heritage rain-forests in Queensland were burned by wildfires [2]. All these facts urge for synergistic efforts from different research communities to develop more efficient fire monitoring, modeling, and control platforms.

Although wildfires that occur in wild-lands are difficult to control, effectively preventing fires from spreading to human habitation can minimize fire hazards drastically. A key requirement to protect residential areas from the wildfire threats is developing precise models that predict the fire spread to guide investing the fire control efforts on more impactful spots. This research proposes a novel data-driven low-complexity fire spread model based on aerial images that incorporates

¹This material is based upon the work supported by the National Science Foundation under Grant No. 1755984.

environmental factors and vegetation density for more accurate fire spread prediction.

Advanced fire spread modeling is a long-lasting research topic. In the last century, a few simple conceptual models were established to predict the fire spread. Fons in 1946 [3], and Emmons in 1963 [4] calibrated the surface fire equilibrium spread rate on flat grounds by combustion experiments in flame chamber and wind tunnel, respectively [3], [4]. The core of their approaches is developing an empirical model of fuel composites under other wind and slope conditions. Afterward, Richards developed a set of functions that characterizes fire front propagation in terms of elliptical shapes [5]. Today some simple empirical models still assume that the fire front propagates in an elliptical shape. With the development of high-performance computing technology, some researchers have made achievements in developing physics-based models in recent years. Two examples include the Wildland Urban Interface Fire Dynamics Simulator developed by the Los Alamos National Laboratory in 2007 [6] and University of Utah's Coupled Atmosphere-Wildland Fire Large Eddy Simulator developed in 2009 [7]. Moreover, the equation-based semiempirical model developed by Rothermel for the USDA forest service has significantly improved the accuracy of empirical models [8].

Most previously reported wildfire models are based on analyzing fire behaviors, processing statistical data, and incorporating physical functions [9]. These models, based on their modeling approaches, can be divided into four categories of (i) empirical models, (ii) semi-empirical models (e.g., Rothermel's model) [9], (iii) statistical models (e.g., Canadian wild-land fire model) and (iv) physical models [10]. The empirical and semi-empirical models process fire behaviors to develop practically meaningful models [11], while the statistical models draw statistical conclusions from the history of fire incidents. Also, physical models focus on developing equations that mimic the impact of different factors on fire spread. Therefore, neither statistical models nor physical models take into account fire behaviors [12]. Neither of the statistic and physical models seems to be practically useful since the former is limited to forests where statistical data is available for a long period of time, and the latter is too complex and rarely applicable. Further, physical models do not incorporate specific geographical, climate and environmental factors readily available for the impacted area. Therefore, our modeling follows the recent trend of developing data-driven empirical and semi-empirical models.

Empirical models utilize simple formulas derived from experiments with a few adjustable parameters which are easy to obtain [11]. Current empirical models typically consider slope direction and fire resistance coefficients of the plants; however, ignore the vegetation density [13]. Another limitation of empirical models is that an accurate fire simulation can only be realized in areas with little topographic changes [11], [13]. Furthermore, empirical models do not consider heat conduction mechanisms [13], so that these models do not define when the fire front would stop in the simulation phase. Indeed, most empirical models assume that the fire fronts always form elliptical shape [11] which is too simplistic and obviously do not provide a reasonably accurate estimate of fire frontline evolution in most cases.

Rothermel's semi-empirical model is a more complex model with 11 parameters [14] including vegetation density. It is based on the spread model of energy conservation, considering the mechanism of heat conduction. Although the Rothermel's model is more flexible than the former empirical models, unfortunately, it does not offer much higher accuracy [15]. We conjecture that the inaccuracy of this model mainly relates to three main problems. First, the model formulation is dependent on the accuracy of the parameters, some of which are difficult to obtain precisely, and some are even unavailable in practice. Second, there exist interlaced and nesting relationships between parameters that cause huge deviations from reality when some of the parameters are not accurate enough [13]. Third, although the model considers the vegetation density with heat conduction mechanisms [16], it assumes that combustibles are uniformly distributed [13] which can be different from the actual situation. In fact, there can be many barriers in the wildfire propagation direction like rivers and highways, which may stop the expansion of wildfire. Therefore, the fire spread models that ignore the region profile and the vegetation distribution do not provide accurate simulations in general.

Our work is the first work, to the best of our knowledge, that considers using image processing to extract the truly spatial distribution of vegetation in the fire region and incorporating it into the spread modeling. The algorithm is applied to different forest types, vegetation, and seasons including forest types with mixed vegetation. We use top-view images taken by different technology including satellites [17], planes [18], and more recently by unmanned aerial vehicles (UAVs) as an emerging low-cost technology [17], [19]–[22].

Once the vegetation profile of the regions is extracted from the top-view aerial images, it is converted into the *cellular automata format* that suits our simulation. This format is grid of cells, each of which associated with three states, defined in sequel.

In the fire spread modeling part, we combine the vegetation distribution with the principle of heat conduction in Rothermel's model, which can reflect the process and the state of the wildfire spread. To construct the model, we choose parameters that significantly affect the fire spread, yet are easily available in practice at a reasonable accuracy. These parameters include the instantaneous speed and direction of the wind averaged over predefined time intervals, fire propagation

rate of combustibles, the vegetation density, and the slope (magnitude of the gradient) as well as the aspect (direction of the maximum gradient magnitude) of the terrain. This model uses the heat conduction as the baseline method while using the above parameters to express the complex phenomenon of fire spread through some macro rules discussed later in this paper.

II. IMAGE PROCESSING METHODOLOGY

Our methodology uses the top-view images for vegetation profiling of the region. This operation is based on determining some points in the image as a *reference* for the regions with vegetation. Then, all the pixels with close-enough pixel values in the feature map are classified as the vegetation versus the background. This enables a dynamic way of image segmentation to develop a vegetation profile of the region.

Most reference-based image segmentation methods utilize the RGB color space for their feature map [23]. Since some pixels in the image are selected as the reference, it can simply identify pixels with similar colors and the color region segmentation can be performed directly through RGB vectors [23]. However, this method is sensitive to the pixel values and may produce false results when some non-vegetation objects present similar feature values to the reference. For instance, ponds, rivers, and other objects with similar color values to the vegetation reference can be falsely classified as vegetation areas if the method solely relies on the RGB color map.

To alleviate this problem, We propose a new methodology that combines color space rules including the RGB rules and the hue, saturation, intensity (HSI) rules with the frequency features to generate a new metric m [23]. Here, the *frequency* is an index that characterizes the intensity of the grayscale changes in the image [23]. The metric m is used to asses the similarity of pixels to the reference region when classifying the image into vegetation versus background segments. Although the non-vegetated regions may have similar colors to the vegetation references in the original image, but they exhibit considerable distinctions in terms of HSI, and spectrum features that facilitates a more accurate classification.

Our implementation includes the following steps. First, the reference region is processed to obtain the original image in RGB space, HSI space, and the frequency spectrum, respectively denoted as I_{RGB} , I_{HSI} , and I_f . Then, following the work in [23], the coordinates [M,N,K] of the pixels in the above images (RGB, HSI and frequency) are extracted. Next, each of the three images are reshaped into 3 dimensional image with M rows and N columns, and K=3, [M,N,3] [23]. After this transformation, the index of all non-zero-valued pixels in the reshaped images are calculated to form the matrix I as the weighted sum of the RGB, HSI and frequency spectrum components.

The matrix I is simply defined as

$$I = \alpha I_{RGB} + \beta I_{HSI} + \gamma I_f, \tag{1}$$

where α , β , and gamma are mixing coefficients with values between 0 and 1, and $\alpha + \beta + \gamma = 1$ to be tuned based on experiments.

Our experiments verified that the matrix I, when obtained as the weighted sum of the RGB, HSI, and frequency spectrum components, can effectively avoid the misclassification issue of the commonly used RGB-based methods. The matrix I is used to calculate the average vector m and the covariance matrix C of the pixels in the vegetation reference area. Next, we calculate the standard deviation of the RGB, HSI, and frequency spectrum components in the reference region as the square root of the summation of the diagonal elements of C [23]. Then, we find T as the maximum value of the elements in the obtained standard deviations in different spaces. Finally, the image is segmented into the vegetation vs background using a similarity metric. Here, we use Mahalanobis distance as a reference for similarity metric [24]) with T as the threshold [23].

The result of the image segmentation is a binary image that represent the vegetation distribution of the region. The segmented image is converted to the *cellular automata format* to be used in the subsequent spread modeling stage.

To asses the performance of the proposed modeling, we use the images from a real-world massive wildfire, Rim fire, which occurred in the California state in the USA in 2013. This fire burned 257,314 acres and cost more than 127 million (2013 USD) [25], [26]. Fig. 1 shows a satellite image where the perimeter of the fire region at a specific time point (August 26, 2013) is shown by a red contour. We also found a satellite image at the same location before this fire (Fig. 2) available from google earth [27]. We will show later in the results section (Fig. 7) that our model is able to reconstruct the fire spread region which highly correlates wit the actual fire region in Fig.1.

Fig. 3 illustrates the image processing results in terms of the extracted vegetation distribution that is converted into the final (*cellular automata*) format. To model the fire spread, we define 3 possible states for each cell, corresponding to No-fire, on-fire, and burned out as explained in Section III.A. Our fire spread model exhibits superior performance for forests where a single tree species is dominant. However, for the forest with diverse tree species, when the color of different vegetation types varies considerably, we take the following approach. We extract multiple vegetation references and use them to segment the vegetation of different colors separately, then we synthesize all segmented images into one picture using majority voting to obtain the most accurate vegetation distribution.

III. FIRE SPREAD MODEL

Since our model modified and complements the Rothermel's model, we first review this model, and then mention how we incorporate the wind and vegetation density into the model.

A. Heat Conduction Model

The Rothermel's surface fire spread model is based on the conservation of energy [9], presuming that the spread of fire fits the Huygens' model [16]. Based on the conservation of energy, we perform the heat conduction mechanisms on modeling the wildfire spread. The heat conduction mechanisms can be represented by a set of simple rules in *cellular automata* as follows [29]. Each vegetation cell has three states, is



Fig. 1: Map of the RIM fire. The red line present the perimeter of the fire region at 2 a.m. PDT, August 26, 2013 [28].



Fig. 2: Google Earth satellite historical image (2013) at same location before the RIM fire [27].

burning/on fire (OF), burned out(BO) and no fire (NF). Rule 1 states that for a cell with current state of n(i,j,t)=OF, its next state is n(i,j,t+1)=BO. Rule 2 states the cell with current state n(i,j,t)=BO remain at the same state n(i,j,t+1)=BO. Rule 3 states that a cell with current state n(i,j,t)=NF and $sum[n(i\pm 1,j\pm 1,t)=OF]>0$, then its next state would be n(i,j,t)=OF. The above rules describe the basic nature of the wildfire spread. These rules defines the spread of fire in which the unburned combustibles in front of the wildfire are continuously ignited.

Since we are using a probabilistic spread model, we change rule 3 as follows. The neighbor cell of a burning cell with n(i,j,t) = OF becomes on fire $n(i\pm 1,j\pm 1,t+1) = OF$, with probability P_f defined to capture the impact of topology, slope, wind, vegetation density as described in the next sections. Also, we add the forth rule that states a cell with state n(i,j,t) = OF transitions to state n(i,j,t+1) = BO if the burning time $t - \operatorname{argmin}_{t'}\{t' < t, \ n(i,j,t') = OF\}$ exceeds a predefined burning time t_B, where t_B depends on the vegetation type of the region.

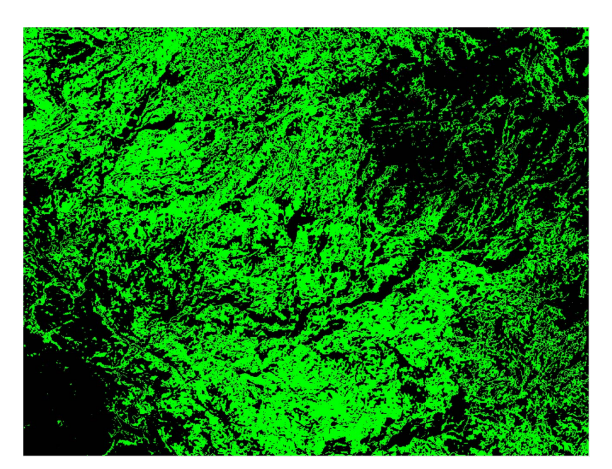


Fig. 3: Image processing result in cellular automata format using the proposed reference-based segmentation algorithm.

B. The influence of topography

Many empirical models suggest that topography is an important factor that affects fire behavior. In the empirical analysis, a flat terrain or positive slope can contribute to the faster fire spread, while an environment with complex terrain and sharp downhills (negative slopes) can slow down the fire spread. A commonly used relationship between the terrain slope and the fire behavior can be defined as [30]:

$$P_s = P_{0s} + P_{1s}\cos(t\theta_s),\tag{2}$$

where P_s represent the fire propagation probability affected by the train slope, P_{0s} is the baseline propagation probability (when the slope is zero), P_{1s} is the slope-dependent propagation probability, θ_s is the slope angle of the patch, and t is an adjustable coefficient that depends on the experiments [29], [30]. For adjacent cells, θ_s is given by:

$$\theta_s = tan^{-1}(\frac{|A_1 - A_2|}{l}),$$
(3)

where A_1 and A_2 are the altitudes of the two cells and l is the side length of the cell (i.e. the distance between the centers of the two adjacent cells).

C. The influence of wind

We also incorporate the impact of the wind on the fire spread. In this respect, we present the wind as a vector field that models the average of instantaneous winds over an interval equivalent to the one time-slot of the simulations.

To model the relationship between the wind and fire propagation, we calculate the probability of fire spread from any cell to its eight adjacent cells under the influence of wind as shown in Fig. 4. The probability P_w of fire propagation to the adjacent cell affected by the wind factor is:

$$P_w = P_{0w} + P_{1w}\cos(a_w\theta_w),\tag{4}$$

where P_{0w} is the baseline propagation probability in no-wind condition, P_{1w} is the wind-dependent propagation probability, θ_w is the direction between the wind and the line connecting the cell to its adjacent cell, and a_w is a tuning parameter. The parameters P_{0w} , P_{1w} , and a_w are obtained from experiments.

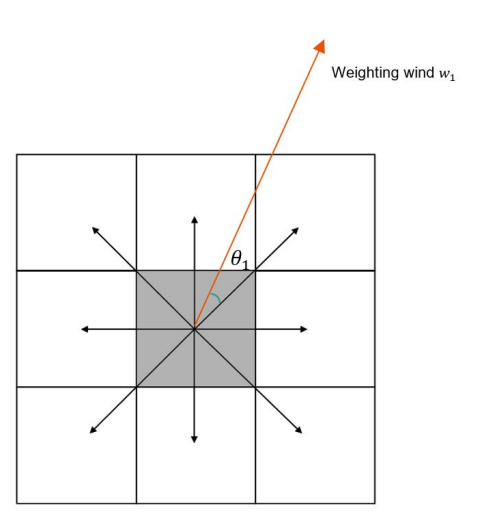


Fig. 4: Weighted wind impact on fire spread using cellular automata fire spread model.

D. The influence of vegetation density

Most methods assume a constant baseline propagation probability that is ignorant of the influence of vegetation density. In reality, the vegetation distribution is not homogeneous, where denser vegetation not only increases the propagation rate, but also provides more burning fuel for longer burning time. This important factor is not considered by former models. Our way of extracting the actual vegetation density enables us to incorporate this important factor into the spread modeling. To this end, we first divide the extracted vegetation image (e.g. Fig. 3) into equally sized 4×4 small tiles, then calculate the maximum connected region for each image tile. The size of the maximum connected region is used as an index vd(i, j) =number of connected pixels/16 that represent the vegetation density of the corresponding cell. Then, the propagation probability of each cell (i, j) is assumed to be proportional to the vegetation density as

$$P_d = P_{0d} * vd, (5$$

where P_{0d} is the baseline propagation probability for full vegetation density vd=1. This is based on a linear relationship between the vegetation density and the propagation probability, and otherwise, 16 distinct spread rates $R_1, R_2, \ldots R_{16}$ can be learned for each vegetation density level based on experiments.

In order to consider all three topology, wind, and density factors, we use

$$P_f(i,j) = P_s(i,j) * P_w(i,j) * P_d(i,j)$$
 (6)

as the effective propagation probability of cell (i, j). Baseline probabilities are used for each factor, if an accurate estimate of the factor is not available.

IV. RESULTS

In this section, we illustrated the *cellular automata* simulation of the Rim fire in the United States to verify the consistency of our fire spread model with real-world incidents. For the comparison with our results, we found the real progressing

of the fire from August 19 through August 27 in 2013 as shown in Fig. 5. Fig. 7 is our simulation results of the fire spread, with parameter values of $t_1 = 0.35$ and $t_1 = 0.55$, t = 0.83, $P_{0w} = 0.1$, $P_{1w} = 0.8$ and a = 0.95. Since the actual wind parameters during the Rim fire in 2013 were not available, we assumed that the wind was constant with a fixed direction by Fig. 6. We determined the direction of the weighted wind in the simulation by revising the direction of the smoke in the above picture (note that we compensate for the orientation difference of the two pictures). The simulation results in Fig. 7 illustrates the estimated fire perimeters at different time points which are similar to the fire progression in Fig. 5. This excellent match verifies the accuracy of our model. This high alignment between the modeling results and reality is consistent. Indeed, we show the fire region for four time- points (64, 106, 181, and 545) in our simulations in Fig. 7, which shows a high consistency with the four time-points in Fig. 5 captured the fire region on Aug.19, Aug.20, Aug.21 and Aug.27.

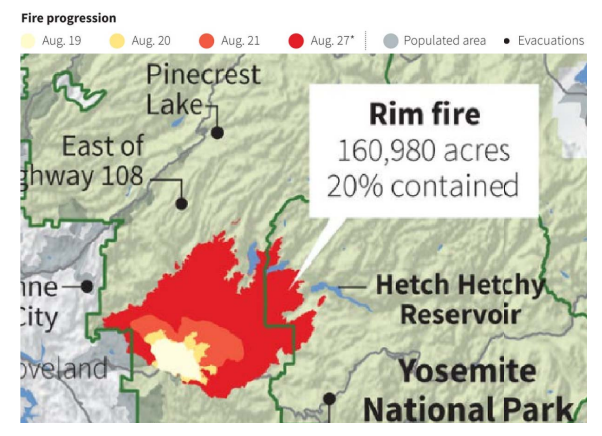


Fig. 5: Rim fire progression from August 19 through August 27, 2013 [31]



Fig. 6: Satellite image of the Rim Fire, on August 23, 2013 [32]

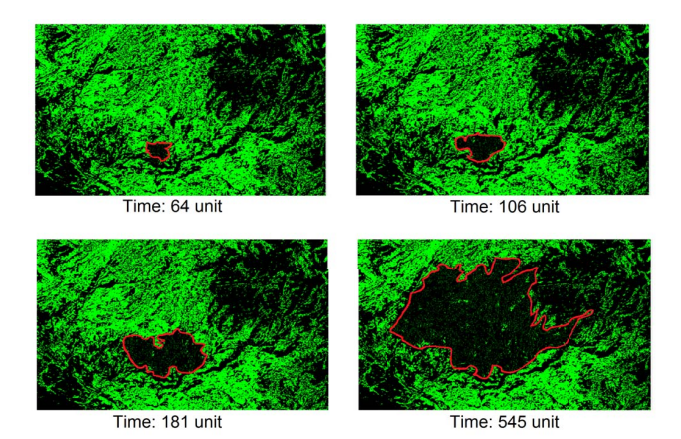


Fig. 7: Prediction of burned area by the proposed model.

V. CONCLUSIONS

This paper implements a new method for forest wildfire propagation modeling that combines empirical fire heat conduction methods and digital image processing for vegetation density estimation. The proposed image processing stage uses top-view images taken by drones, which provide flexibility and convenience compared to traditional fire field parameter acquisition methods. Through the proposed image processing algorithm, the true distribution of the vegetation density is obtained and incorporated into the probabilistic fire spread modeling. Despite the physical and statistical models, our method is applicable to forests with mixed vegetation and different climate conditions provided that the model parameters are learned based on experiments. Our model is lowcomplexity and can be run by drones on the fly to adjust the model parameters. We applied the model to the California Rim fire region, and the results show a perfect match with the actual fire spread data, available online.

REFERENCES

- [1] N. F. P. Association, "wildfire." NFPA.
- [2] C. for Disaster Philanthropy, "2019-2020 australian bushfires." CDP, 2020.
- [3] L. WALLACE, "Analysis of fire spread in light forest fuels," *Journal of Agricultural Research*, vol. 72, no. 3, p. 93, 1946.
- [4] H. W. Emmons, "Fundamental problems of the free burning fire," in *Symposium (International) on Combustion*, vol. 10, no. 1. Elsevier, 1965, pp. 951–964.
- [5] G. D. Richards, "An elliptical growth model of forest fire fronts and its numerical solution," *International journal for numerical methods in engineering*, vol. 30, no. 6, pp. 1163–1179, 1990.
- [6] W. Mell, M. A. Jenkins, J. Gould, and P. Cheney, "A physics-based approach to modelling grassland fires," *International Journal of Wildland Fire*, vol. 16, no. 1, pp. 1–22, 2007.
- [7] R. Sun, S. K. Krueger, M. A. Jenkins, M. A. Zulauf, and J. J. Charney, "The importance of fire-atmosphere coupling and boundary-layer turbulence to wildfire spread," *International Journal of Wildland Fire*, vol. 18, no. 1, pp. 50–60, 2009.
- [8] R. C. Rothermel, A mathematical model for predicting fire spread in wildland fuels. Intermountain Forest and Range Experiment Station, Forest Service, United ..., 1972, vol. 115.
- [9] J. H. Scott, Standard fire behavior fuel models: a comprehensive set for use with Rothermel's surface fire spread model. US Department of Agriculture, Forest Service, Rocky Mountain Research Station, 2005.

- [10] L. M. Johnston and M. D. Flannigan, "Mapping canadian wildland fire interface areas," *International Journal of Wildland Fire*, vol. 27, no. 1, pp. 1–14, 2018.
- [11] G. D. Richards, "The properties of elliptical wildfire growth for time dependent fuel and meteorological conditions," *Combustion science and technology*, vol. 95, no. 1-6, pp. 357–383, 1993.
- [12] C. Tymstra, R. Bryce, B. Wotton, S. Taylor, O. Armitage et al., "Development and structure of prometheus: the canadian wildland fire growth simulation model," Natural Resources Canada, Canadian Forest Service, Northern Forestry Centre, Information Report NOR-X-417. (Edmonton, AB). 2010.
- [13] Y. H. Shuangxi M, B. Z *et al.*, "Improvement of the forest fire simulation algorithm based on the rothermel model," *CNKI*, vol. 10, no. 6, pp. 14–21, 2013.
- [14] R. A. Wilson, Reexamination of Rothermel's fire spread equations in nowind and no-slope conditions. US Department of Agriculture, Forest Service, Intermountain Forest and Range ..., 1990, vol. 434.
- [15] E. Catchpole, M. E. Alexander, and A. Gill, "Elliptical-fire perimeterand area-intensity distributions," *Canadian Journal of Forest Research*, vol. 22, no. 7, pp. 968–972, 1992.
- [16] L. Cunbin, Z. Jing, T. Baoguo, and Z. Ye, "Analysis of forest fire spread trend surrounding transmission line based on rothermel model and huygens principle," *International Journal of Multimedia and Ubiquitous Engineering*, vol. 9, no. 9, pp. 51–60, 2014.
- [17] M. A. Crowley, J. A. Cardille, J. C. White, and M. A. Wulder, "Generating intra-year metrics of wildfire progression using multiple open-access satellite data streams," *Remote Sensing of Environment*, vol. 232, p. 111295, 2019.
- [18] R. S. Allison, J. M. Johnston, G. Craig, and S. Jennings, "Airborne optical and thermal remote sensing for wildfire detection and monitoring," *Sensors*, vol. 16, no. 8, p. 1310, 2016.
- [19] A. Razi, "Optimal measurement policy for linear measurement systems with applications to uav network topology prediction," *IEEE Transac*tions on Vehicular Technology, 2019.
- [20] S. Islam, Q. Huang, F. Afghah, P. Fule, and A. Razi, "Fire frontline monitoring by enabling uav-based virtual reality with adaptive imaging rate," in *Asilomar Conference on Signals, Systems, and Computers*, 2019.
- [21] S. Islam and A. Razi, "A path planning algorithm for collective monitoring using autonomous drones," in 2019 53rd Annual Conference on Information Sciences and Systems (CISS). IEEE, 2019, pp. 1–6.
- [22] H. Wu, H. Li, A. Shamsoshoara, A. Razi, and F. Afghah, "Transfer learning for wildfire identification in uav imagery," in 2020 54th Annual Conference on Information Sciences and Systems (CISS). IEEE, 2020, pp. 1–6.
- [23] R. C. Gonzalez, R. E. Woods, and S. L. Eddins, Digital image processing using MATLAB. Pearson Education India, 2004.
- [24] A. N. Benaichouche, H. Oulhadj, and P. Siarry, "Improved spatial fuzzy c-means clustering for image segmentation using pso initialization, mahalanobis distance and post-segmentation correction," *Digital Signal Processing*, vol. 23, no. 5, pp. 1390–1400, 2013.
- Processing, vol. 23, no. 5, pp. 1390–1400, 2013.

 [25] InciWeb. (2013) Rim fire. [Online]. Available: https://en.wikipedia.org/wiki/Rim_Firecite_note 6
- [26] N. News. (2013) California's third-largest wildfire fills yosemite valley with smoke on holiday weekend.
- [27] . C. S. Google Earth Pro. (2020) Historical imagery. [Online]. Available: https://www.google.com/earth/versions/download-pro
- [28] B. Gabbert. (2013) California: Rim fire at yosemite np. [Online]. Available: https://wildfiretoday.com/2013/08/21/california-rim-fire-west-of-yosemite-np
- [29] A. Alexandridis, D. Vakalis, C. I. Siettos, and G. V. Bafas, "A cellular automata model for forest fire spread prediction: The case of the wildfire that swept through spetses island in 1990," *Applied Mathematics and Computation*, vol. 204, no. 1, pp. 191–201, 2008.
- Computation, vol. 204, no. 1, pp. 191–201, 2008.

 [30] D. R. Weise and G. S. Biging, "Effects of wind velocity and slope on flame properties," Canadian Journal of Forest Research, vol. 26, no. 10, pp. 1849–1858, 1996.
- pp. 1849–1858, 1996.
 [31] J. Weisenthal. (2013) This map shows how rapidly the yosemite wildfire has spread in just over a week. [Online]. Available: https://www.businessinsider.com/this-map-shows-how-rapidly-the-yosemite-wildfire-spread-in-just-over-a-week-2013-8
- [32] N. E. Observatory. (2013) Rim fire, california. [Online]. Available: https://earthobservatory.nasa.gov/images/81936/rim-fire-california